A semiclassical wave packet model for the investigation of elastic and inelastic gas–surface scattering

P. M. Agrawal and L. M. Raff

Citation: The Journal of Chemical Physics **77**, 3946 (1982); doi: 10.1063/1.444348
View online: http://dx.doi.org/10.1063/1.444348
View Table of Contents: http://scitation.aip.org/content/aip/journal/jcp/77/8?ver=pdfcov
Published by the AIP Publishing

A semiclassical wave packet model for the investigation of elastic and inelastic gas–surface scattering

P. M. Agrawal

Department of Physics, Government College, Ajmer (Rajasthan), India

L. M. Raff

Department of Chemistry, Oklahoma State University, Stillwater, Oklahoma 74078
(Received 17 May 1982; accepted July 1982)

A semiclassical wave packet model that permits simultaneous study of surface diffraction, Debye–Waller effects, and inelastic energy transfer processes at the gas–surface interface is presented. The incident atomic beam is represented by a quantum mechanical wave packet whose momentum-space probability density corresponds to that employed in the molecular-beam experiments being simulated. A semiclassical forced-oscillator-type approximation couples the surface motion to that of the wave packet through a time-varying potential obtained from a solution of Hamilton's equations of motion for the lattice. Explicit integration procedures are used to evolve the wave packet through this time-varying field. The average final kinetic energy of the beam, the angular distributions and diffraction patterns, Debye–Waller broadening effects, and the surface phonon spectrum are obtained from the scattered wave packet and its Fourier transform. The model has been applied to the case of an atomic hydrogen beam having a square distribution of incident momenta impinging upon a simple two-dimensional lattice. The results yield diffraction patterns that correlate with the known grating of the lattice. The average final kinetic energy of the beam is found to vary linearly with incident energy and with surface temperature in accord with the results of recent molecular beam experiments, and a surface phonon spectrum that exhibits one-, two-, and three-phonon processes is obtained.

I. INTRODUCTION

As molecular-beam gas–surface experiments become more sophisticated, an increasing amount of information related to inelastic and reactive processes occurring at the gas–surface interface is becoming available.[1] For example, Janda *et al.*[2] have recently reported measurements of the velocity distributions of Ar atoms scattered from a polycrystalline tungsten surface. These measurements have allowed them to relate the average kinetic energy of exiting Ar atoms $\langle E_e \rangle$ to the average incident kinetic energy $\langle E_i \rangle$ and to the surface temperature T_s. Over a wide range of values, they observe a linear relationship between these quantities. That is,

$$\langle E_e \rangle = \alpha_g \langle E_i \rangle + \alpha_s 2k_B T_s \,, \tag{1}$$

where k_B is Boltzmann's constant and α_g and α_s are coefficients that do not depend upon $\langle E_i \rangle$ or T_s. For the particular case of an Ar beam incident on polycrystalline tungsten at an incidence angle $\theta_i = 45°$ and for observation in the specular direction, Janda *et al.*[2] observe $\alpha_g = 0.83$ and $\alpha_s = 0.20$. For lighter atom scattering from clean, single crystal surfaces, we may expect to see experimental information related to quantum effects, such as discrete surface phonon spectra, becoming increasingly available.

The rapid advance of experimental studies of inelastic and reactive gas–surface processes has been matched by a simultaneous advance of theoretical methods that permit the investigation of such interactions. For example, Adelman and Doll[3] have adapted the generalized Langevin equation (GLE) to the study of inelastic gas–surface processes. In this procedure, the coupling between the incident atom and a small group of surface atoms is explicitly included in the formulation, while the effects of the remainder of the surface are described by a friction kernal and a random force. Shugard, Tully, and Nitzan[4] have utilized this approach to treat energy transfer and sticking probabilities in a (He–W) system. Corrugated "hard" and "soft" wall models have been developed to treat elastic scattering and diffraction effects.[5] Recently, Kumamoto and Silbey[6] have used a semiclassical approach in which a time-dependent surface Hamiltonian is obtained from a classical atom trajectory. By using a superposition of surface states as the initial surface state, they were able to obtain results for energy transfer and sticking probabilities that were dependent upon T_s.

For cases in which quantum effects are minimal, classical trajectory simulation of the gas–surface encounter using detailed lattice models have proven to be very accurate. For example, Lorenzen and Raff[7] have recently reported velocity distributions for [Ar–W(110)] scattering originally calculated by trajectory methods in 1970, that are in good accord with those recently measured by Janda *et al.*[2]

Although the combination of these methods allows most elastic and inelastic scattering processes to be treated in detail, no one method can treat the full range of diffraction and Debye–Waller effects, inelastic energy transfer that includes discrete phonon transfer, as well as bound-state resonance effects. A full-quantum mechanical model that would permit the study of all of these is clearly a desirable goal. Unfortunately, a purely quantum-mechanical description of gas–surface scattering is very difficult to formulate due to the presence of strong couplings, low velocities, and the number of scattering channels that must be considered. However, semiclassical models that treat part of problem classi-

 0021-9606/82/203946-07$02.10

cally and part quantum mechanically are feasible. The recent studies of Kumamoto and Silbey[6] are an excellent example.

In this paper we present the details of a semiclassical model of gas–surface scattering that permits the investigation of both elastic and inelastic processes. The incident atomic beam is treated as a wave packet moving in a time-varying potential field created by the classical motion of the lattice atoms. Since a quantum mechanical wave packet has a built-in distribution of both positions and momenta, it is possible to replace the study of the statistical average behavior of many classical trajectories by evolving an appropriately chosen single wave packet.[8] In addition, quantum effects, such as diffraction and resonant energy transfer, are properly described.

The model permits the use of any gas–surface potential desired. Alternatively, a parametrized potential may be employed and the model used as a means to deconvolute molecular-beam scattering results. The lattice representation may be realistic, detailed, and three dimensional. It may possess the translational symmetry of a perfect crystal or have lattice defects and impurities, as desired. The incident atomic beam possesses the in-plane velocity distribution and incidence angle present in the actual beam experiments being simulated. The results of the calculations yield diffraction patterns and, in principle, Debye–Waller factors. Inelastic phonon energy transfer and the resulting phonon spectra are obtained directly. The details of the formulation are given in Sec. II.

As an illustrative example, we have applied this semiclassical wave packet model to the investigation of elastic and inelastic scattering of an atomic hydrogen beam from a two-dimensional lattice. The results of this study are given in Sec. III.

II. FORMULATION

The incident atomic beam is represented by a wave packet $\psi(x,y,t)$ moving in the plane described by surface normal and the incident velocity vector. We take this plane to be the $(x-y)$ plane. The time evolution of $\psi(x,y,t)$ is described by

$$\mathcal{H}\psi(x,y,t)=i\hbar\,\partial\,\psi(x,y,t)/\partial t\ , \tag{2}$$

with

$$\mathcal{H}=(-\hbar^2/2m)[\partial^2/\partial x^2+\partial^2/\partial y^2]+V(x,y,Q)\ . \tag{3}$$

The interaction potential $V(x,y,Q)$ at point (x,y) is dependent upon the instantaneous positions of all of the lattice atoms. The set of coordinates specifying these positions is denoted by Q. In principle, $V(x,y,Q)$ may have any form. However, in most gas–surface studies that have been published to date, $V(x,y,Q)$ is usually assumed to have a pairwise form

$$V(x,y,Q)=\sum_i V_i(x,y,X_i^{\mathcal{L}},Y_i^{\mathcal{L}})\ , \tag{4}$$

where V_i represents the potential at point (x,y) due to the ith lattice atom whose position is given by $(X_i^{\mathcal{L}},Y_i^{\mathcal{L}})$. The lack of information concerning the appropriate form of $V(x,y,Q)$ is generally responsible for the use of a simple pairwise potential such as Eq. (4). This lack of knowledge concerning $V(x,y,Q)$ is undoubtedly the major bottleneck in the theoretical investigation of surface processes.

In order to simplify the scattering problem in a way that still permits the investigation of diffractive scattering and inelastic resonant energy transfer, we now invoke a semiclassical approximation analogous to that of a forced-oscillator model. The lattice motion is assumed to be classical and unperturbed by the incident atomic beam. Solution of Hamilton's equations thus yields $X_i^{\mathcal{L}}$ and $Y_i^{\mathcal{L}}$ as functions of time. Direct substitution into Eq. (4) converts $V(x,y,Q)$ into a time-varying function

$$V(x,y,t)=\sum_i V_i[x,y,X_i^{\mathcal{L}}(t),Y_i^{\mathcal{L}}(t)]\ . \tag{5}$$

The effect of surface temperature enters through its effect upon the amplitude of the oscillations of the classical lattice. In principle, the results of the wave packet calculations using Eq. (5) should be averaged over the entire initial phase–space available to the surface. In practice, however, a complete phase averaging will probably move the computational requirements of the model outside the range of available computer time. As a consequence, integration of the results over the ensemble of initial surface states will either have to be limited or suppressed entirely.

Although this semiclassical approximation is similar in form to that of a forced-oscillator model, the inaccuracies inherent in it are probably not as great. In the forced-oscillator model, an elastic atomic trajectory perturbs a quantum oscillator. The effects of inelastic energy transfer upon the incident atom are ignored. Consequently, when the energy transfer cross sections become large, this neglect can produce a significant error in the results. In the present model, the situation is reversed. A classical lattice trajectory perturbs an incident quantum wave packet. In a manner analogous to the forced-oscillator model, the effects of energy transfer upon the lattice are ignored in computing the lattice trajectory. However, since the total energy of the lattice is significantly larger than that involved in the inelastic transfer, the error associated with the neglect of this transfer will generally be smaller than is the case when the transfer is ignored relative to the energy of the incident atom.

The initial wave packet $\psi(x,y,0)$ is chosen such that its Fourier transform yields the momentum distribution present in the incident atomic beam. If this distribution is known from actual TOF measurements or otherwise, numerical methods may be utilized to invert the transformation to yield $\psi(x,y,0)$.

The wave packet is evolved in time using the explicit integration method of Harmuth[9] as extended to two dimensions by Askar and Cakmak.[10] We have previously employed this procedure to study gas–phase collinear exchange reactions[11] and have found it to be faster than implicit integration methods.

The scattered wave packet $\psi(x,y,\infty)$ contains all the information regarding the scattered atomic beam. The following quantities may be easily computed:

Average final kinetic energy $\langle E_e \rangle$

$$\langle E_e \rangle = \int\int \psi^*(x,y,\infty) \times [-\hbar^2/2m(\partial^2/\partial x^2 + \partial^2/\partial y^2)]\psi(x,y,\infty)dx\,dy \ . \quad (6)$$

In the numerical calculations, the required derivatives are evaluated by second difference methods

$$\partial^2\psi(x,y,\infty)/\partial x^2 = (\psi_{i+1,j} + \psi_{i-1,j} - 2\psi_{i,j})/\Delta x^2 \ , \quad (7)$$

where ψ_{ij} denotes the value of $\psi(x,y,\infty)$ at grid point (i,j), and Δx is the grid spacing along the x direction. A similar procedure is employed to obtain $\partial^2\psi(x,y,\infty)/\partial y^2$.

Probability density (ρ) *and probability current density* (**S**):

$$\rho = \psi^*\psi \quad (8)$$

and

$$\mathbf{S} = (\hbar/2mi)[\psi^*\nabla\psi - (\nabla\psi^*)\psi] \ . \quad (9)$$

Taking components, we obtain

$$S_x = (\hbar/m)[\psi_R \partial\psi_I/\partial x - \psi_I \partial\psi_R/\partial x] \ , \quad (10)$$

$$S_y = (\hbar/m)[\psi_R \partial\psi_I/\partial y - \psi_I \partial\psi_R/\partial y] \ , \quad (11)$$

where ψ_R and ψ_I are the real and imaginary components of $\psi(x,y,\infty)$. Equations (8)–(11) give the angular distribution of the scattered beam.

Energy distribution: The final energy distribution of scattered wave packet in the field-free region, where the total energy is just the kinetic energy, can be obtained by computation of the Fourier transform of $\psi(x,y,\infty)$, $\theta(k_x,k_y)$. (For brevity, we shall herewith drop the specification $t\to\infty$):

$$\theta(k_x,k_y) = [2\pi]^{-1} \times \int_y\int_x \exp[-i(k_x x + k_y y)]\psi(x,y)dx\,dy \ . \quad (12)$$

Separation into real and imaginary parts gives

$$\theta_R(k_x,k_y) = (2\pi)^{-1}\int_y\int_x [\psi_R(x,y)\cos(k_x x + k_y y) + \psi_I(x,y)\sin(k_x x + k_y y)]dx\,dy \quad (13)$$

and

$$\theta_I(k_x,k_y) = [2\pi]^{-1}\int_y\int_x [\psi_I(x,y)\cos(k_x x + k_y y) - \psi_R \sin(k_x x + k_y y)]dx\,dy \ . \quad (14)$$

The probability that the x component of momentum lies in the range $\hbar k_x \le P_x \le (k_x + dk_x)\hbar$ while the y component lies in the range $\hbar k_y \le P_y \le (k_y + dk_y)\hbar$ is equal to $|\theta(k_x,k_y)|^2 dk_x\,dk_y$. From the momentum-space diagram shown in Fig. (1), we see that

$$P(k)dk = \int_{\theta_k=0}^{2\pi} |\theta(k,\theta_k)|^2 k\,dk\,d\theta_k \ , \quad (15)$$

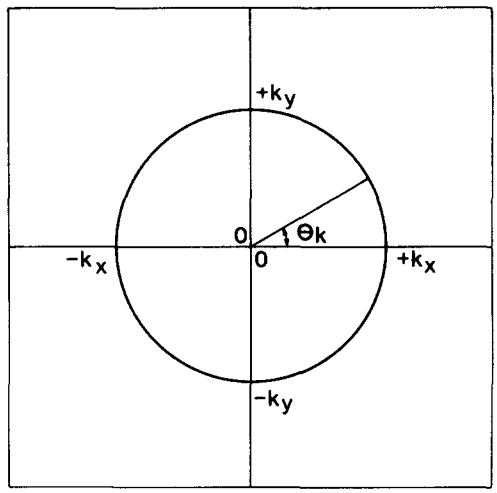

FIG. 1. Two-dimensional momentum space. The circle represents the locus of all points corresponding to the same energy $E_k = \hbar^2 k^2/2m$.

where $P(k)dk$ is the probability that the energy lies in the range $E_k \le E \le E_k + dE_k$, with

$$E_k = \hbar^2 k^2/2m \ , \quad (16)$$

$$\theta(k,\theta_k) = \theta(k_x,k_y) \ , \quad (17)$$

$$k = [k_x^2 + k_y^2]^{1/2} \ , \quad (18)$$

and

$$\theta_k = \tan^{-1}[k_y/k_x] \ . \quad (19)$$

III. ILLUSTRATIVE EXAMPLE

As an illustrative example, we have applied the semiclassical wave packet model to the case of an atomic hydrogen beam incident upon a two-dimensional surface at angle θ_i.

The initial wave packet is taken to be

$$\psi(x,y,0) \equiv \psi_0(x,y) = G(q_1)F(q_2) \ , \quad (20)$$

where

$$q_1 = X\cos\theta_i + Y\sin\theta_i \quad (21)$$

and

$$q_2 = Y\cos\theta_i - X\sin\theta_i \ , \quad (22)$$

with

$$X = x - x_0 \ , \quad \text{and } Y = y - y_0 \ . \quad (23)$$

In Fig. (23), (x_0, y_0) are the coordinates of atom C in the surface (see Fig. 2). We have chosen

$$G(q_1) = \frac{\exp(-ik_0 q_1)\sin[\Delta k(q_1 - q_1^0)]}{(q_1 - q_1^0)[\pi(\Delta k)]^{1/2}} \quad (24)$$

and

$$F(q_2) = \begin{cases} (2a)^{-1/2} \ , & \text{for } (-a \le q_2 \le a) \ , \\ 0 \ , & \text{for } q_2 > a \text{ or } q_2 < -a \ , \end{cases}$$

where

$$a = [R_e/2.0 + \Delta y]\cos\theta_i \ . \quad (26)$$

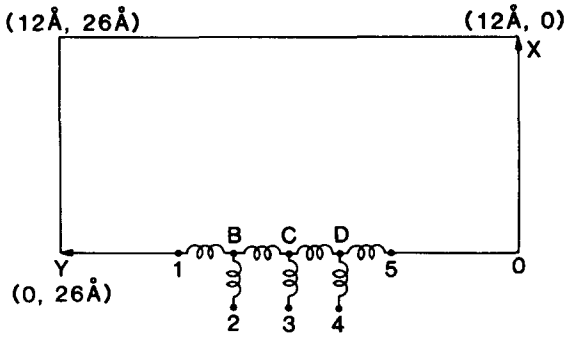

FIG. 2. Configuration space and two-dimensional lattice model. B, C, and D represent movable lattice sites of mass 20 amu. Points 1, 2, 3, 4, and 5 represent fixed sites of infinite mass.

In Eq. (26), R_e is the equilibrium lattice spacing.

The Fourier transform of $G(q_1)$ is

$$g(k)=\begin{cases}\exp(ikq_1^0)/[2\Delta k]^{1/2}, & \text{for } (k_0-\Delta k)\le k\le(k_0+\Delta k),\\ 0, & \text{for } k>(k_0+\Delta k),\\ & \text{or } k<(k_0-\Delta k).\end{cases} \quad (27)$$

Thus, $G(q_1)$ has a square distribution in momentum space. $F(q_2)$ is a square wave packet in q_2 space with width $2a$. This corresponds to the classical trajectory case of gaseous atoms impinging with equal probability such that their aiming points lie between the midpoint of $\overline{BC}$ and that of $\overline{CD}$ (see Fig. 2).

Finally, we specify the initial location of the incident wave packet by taking $q_1^0=8$ Å. This is sufficiently large to place most of the probability density at $t=0$ outside the effective range of the gas–surface interaction potential. We specify the width of the momentum distribution by taking $\Delta k=0.9$ Å^{-1}. A perspective plot of $|\psi(x,y,0)|^2$, is shown in Fig. 3 for the case of normal incidence.

The lattice, shown in Fig. 2, is a two-dimensional ensemble of three movable atoms B, C, and D with mass

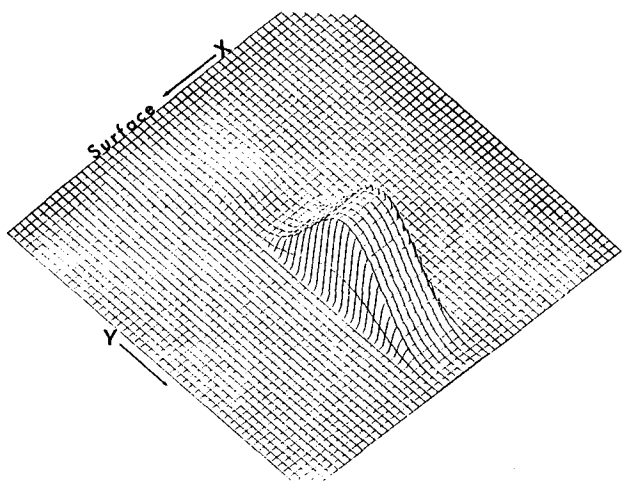

FIG. 3. Probability density $|\psi(x,y,0)|^2$ evaluated over configuration space at $t=0$ with $\theta_i=0°$, $T_s=1500$ K, $\langle E_i\rangle=0.089$ eV.

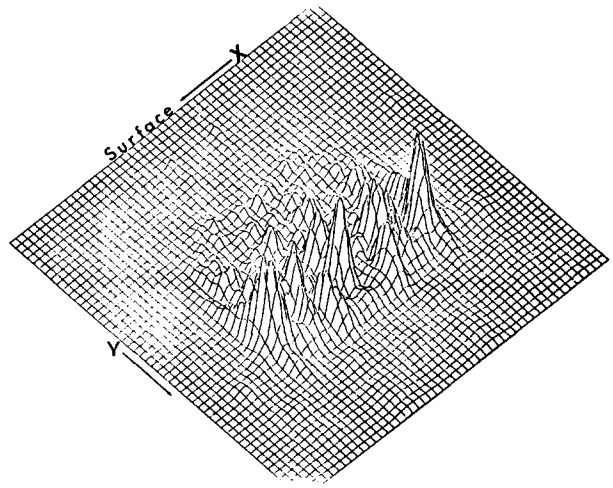

FIG. 4. Scattered probability density evaluated over configuration space for the initial wave packet shown in Fig. 3.

20 amu attached to five sites of infinite mass represented by points 1–5. All adjacent lattice sites are assumed to be connected by harmonic springs whose force constant was taken to be 5.36 eV/Å^2 with an equilibrium spacing of 3.517 Å. Figure 2 also shows the configuration space over which $\psi(x,y,t)$ is evolved. This is a two-dimensional space with an area of 312 Å^2 which includes all space in the range $(0\le y\le 26$ Å) and $(0\le x\le 12$ Å). Outside this configuration space the potential is assumed to be infinite. This assumption makes $\psi(x,y,t)=0$ for $(0<x$ or $y)$ or $x>12$ Å or $y>26$ Å. As a consequence of the finite size employed for this configuration space, it is necessary that the scattering from the surface be essentially complete at a time sufficiently short to prevent reflection of the wave packet from the infinite potential boundaries. For the present application, the 12 $\times$26 Å space is sufficiently large to meet this requirement. Different systems may, of course, require larger configuration–space grids.

The atom–surface interaction potential was assumed to have the pairwise form of Eq. (5), where the V_i are LJ (12, 6) potentials with $\sigma=2.74$ Å and $\epsilon/k_B=38.5$ K. In the present example, the initial surface state was taken to be the symmetric set of outer classical turning points with the initial surface energy equipartitioned into all pairwise bonds. Phase averaging over initial surface states has been omitted.

$\psi(x,y,t)$ has been computed over a 12$\times$26 Å grid in (x,y) space. An equispaced mesh of grid points with $\Delta x=\Delta y=0.2$ Å has been employed with $\Delta t=4\times10^{-16}$ s. For $\langle E_i\rangle=0.095$ eV, an evolution time of 1000 Δt was found to be sufficient. For collisions with larger values of $\langle E_i\rangle$, a smaller number of time steps were required.

Figure 4 shows the predicted spatial distribution $|\psi(x,y,t\to\infty)|^2$ for normal incidence with $T_s=1500$ K and $\langle E_i\rangle=0.089$ eV. The diffraction pattern is evident. The position of the maxima may be easily correlated with the known diffraction grating of the lattice. The diffraction peaks are diffuse rather than sharp due to

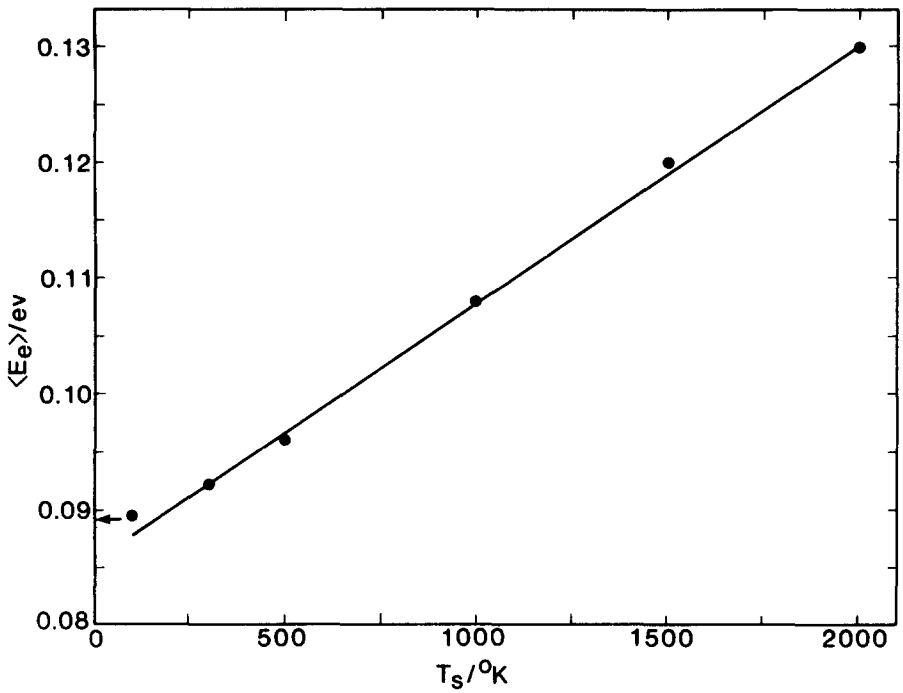

FIG. 5. Variation of $\langle E_e \rangle$ with surface temperature with $\theta_i = 0°$. Horizontal arrow indicates the value of $\langle E_i \rangle$.

the spread of wavelengths in the incident beam and to the thermal motion of the lattice. In principle, it should be possible to compute Debye–Waller factors from a complete analysis of these effects.

Figure 5 shows the variation of $\langle E_e \rangle$ with surface temperature T_s in the range $100 \leq T_s < 2000$ K for a fived value of $\langle E_i \rangle$ indicated by the horizontal arrow in the graph with $\theta_i = 0°$. In Fig. 6 the variation of $\langle E_e \rangle$ with $\langle E_i \rangle$ in the range $0.064 \leq \langle E_i \rangle \leq 0.112$ eV with $\theta_i = 0°$ and $T_s = 1500$ K is given. Figure 7 gives the combined effect. The linear variations obtained in Figs. 5–7 clearly support the recent observations by Janda *et al.*[2] that $\langle E_e \rangle$ depends upon $\langle E_i \rangle$ and T_s in the linear fashion given by Eq. (1).

We have also investigated the behavior of the system for $\theta_i = 30°$, 45°, and 60°. Figures 8–10 show the computed variation of $\langle E_e \rangle$ with T_s in each of these cases. In all cases, the results conform to the Janda *et al.*[2] observation of Eq. (1). The values of α_g and α_s are, however, found to be angle dependent (see Table I).

For Ar incident upon a polycrystalline tungsten surface with $\theta_i = 45°$ and with the measurements being made at the specular angle, Janda *et al.*[2] found $\alpha_g = 0.83$ and $\alpha_s = 0.20$. Thus, the results of Table I show the computed values for these coefficients to be of the right magnitude. Quantitative agreement would not be expected due to the significant differences between the incident atomic beam and surface employed in the calculations and that used in the beam experiments. In addition, we

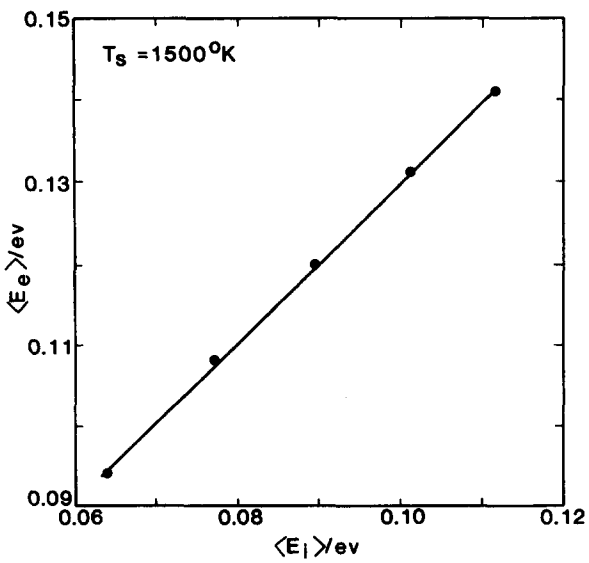

FIG. 6. Variation of $\langle E_e \rangle$ with $\langle E_i \rangle$ for normal incidence with $T_s = 1500$ K.

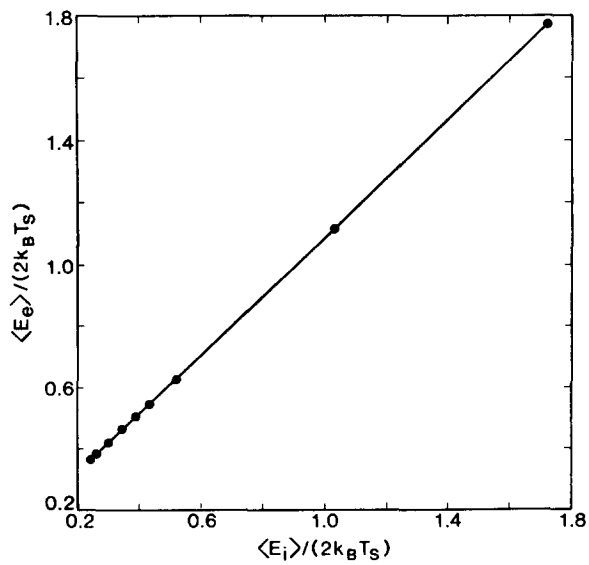

FIG. 7. $\langle E_e \rangle / (2 k_b T_s)$ vs $\langle E_i \rangle / (2 k_b T_s)$ for normal incidence.

compute $\langle E_e \rangle$ by averaging over all scattering angles, whereas the beam measurements are made at the specular angle.

Recently, Grimmelmann *et al.*[12] have shown that the hard-cube model also leads to the linear relationship given in Eq. (1). Their treatment also involves averaging over all scattering angles. However, the hard-cube results predict that only α_g is angle dependent whereas the present wave packet studies predict an angle dependence for both α_g and α_s.

Figure 11 shows the computed surface spectrum obtained from Eqs. (12)–(19) with $T_s = 1500$ K, $\theta_i = 0°$, and $\langle E_i \rangle = 0.089$ eV. The dashed curve in the figure gives the initial distribution of momenta using the scale on the right. The one-, two-, and three-phonon processes for energy transfer from the lattice to the scattered hydrogen-atom beam are evident. The one-phonon transfer from the beam to the lattice is also very intense. The two-phonon transfer to the lattice appears as a small shoulder. For this system, most of the scattering is inelastic. It can be easily shown that the spacings between the maxima of the scattered momentum distribution correlate to the lattice frequencies obtained from a normal mode analysis of the lattice shown in Fig. 2.

IV. SUMMARY

We have presented the details of a semiclassical wave packet model that permits simultaneous study of surface diffraction, Debye–Waller effects, and inelastic energy transfer. The incident atomic beam is represented by a quantum mechanical wave packet whose momentum-space probability density corresponds to that employed in the beam experiments being simulated. The wave packet motion and that of the lattice are coupled semiclassically using an approximation analogous to that of a forced-oscillator model. The motion of the surface is treated classically. Solution of Hamilton's equations yields the position coordinates of all lattice atoms as functions of time, and direct substitution of these functions gives a time-varying potential. Explicit integration methods are employed to evolve the wave packet in this time-varying field.

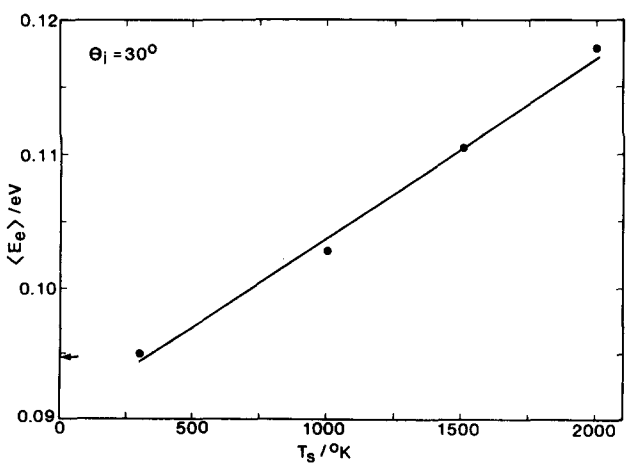

FIG. 8. Variation of $\langle E_e \rangle$ with T_s for $\theta_i = 30°$. Horizontal arrow indicates $\langle E_i \rangle$.

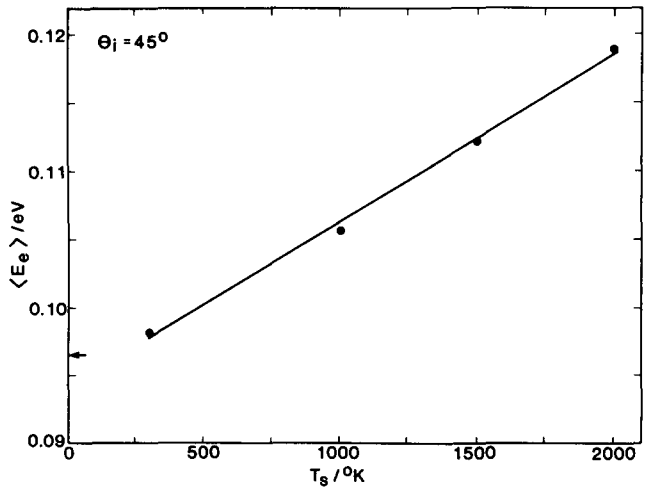

FIG. 9. Same as Fig. 8 for $\theta_i = 45°$.

The scattered wave packet contains all pertinent information with regard to both elastic and inelastic processes at the surface. These include the average final kinetic energy of the beam, the angular distributions and diffraction patterns, if present, spatial broadening due to Debye–Waller effects, and the surface phonon spectra if the surface quanta are sufficiently large to produce a discrete spectrum. Each of these effects may be examined as a function of incidence angle, initial beam "temperature," and surface temperature. In principle, the model could also be used to examine the consequences of lattice defects or surface impurities.

For illustrative purposes, we have applied the model to the case of an atomic hydrogen beam having a square distribution of incident momenta impinging upon a simple two-dimensional lattice. The scattered spatial probability density exhibits a series of diffraction peaks whose angular positions correlate with the known lattice spacings. These diffraction maxima are broad and somewhat diffuse due to the spread of wavelengths present in the incident atomic beam and to the Debye–Waller effect produced by the surface motion. The average final kinetic energy of the beam is found to exhibit a linear dependence upon the initial average kinetic energy and upon the surface temperature in accord with recent molecular-beam results obtained by Janda *et al.*[2] The linear coefficients, however, are found to vary with incidence angle. Finally, we have been able to extract

TABLE I. Dependence of α_g and α_s on angle of incidence θ_i, as measured from the surface normal.

θ_i	α_g	α_s
0°	0.96	0.13
30°	0.96	0.08
45°	0.97	0.07
60°	1.03	0.10

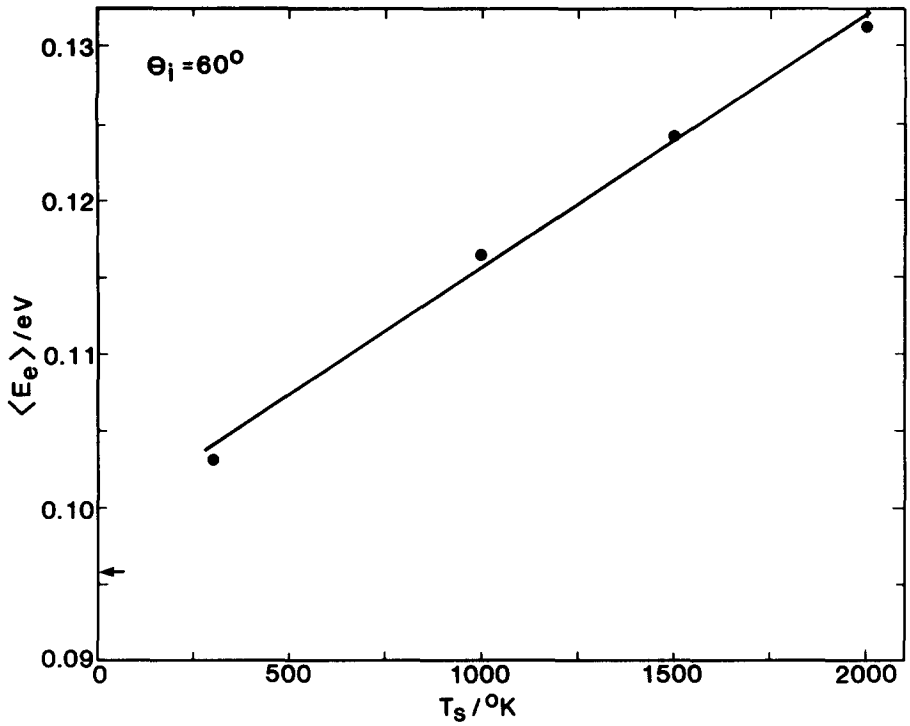

FIG. 10. Same as Fig. 8 for $\theta_i = 60°$.

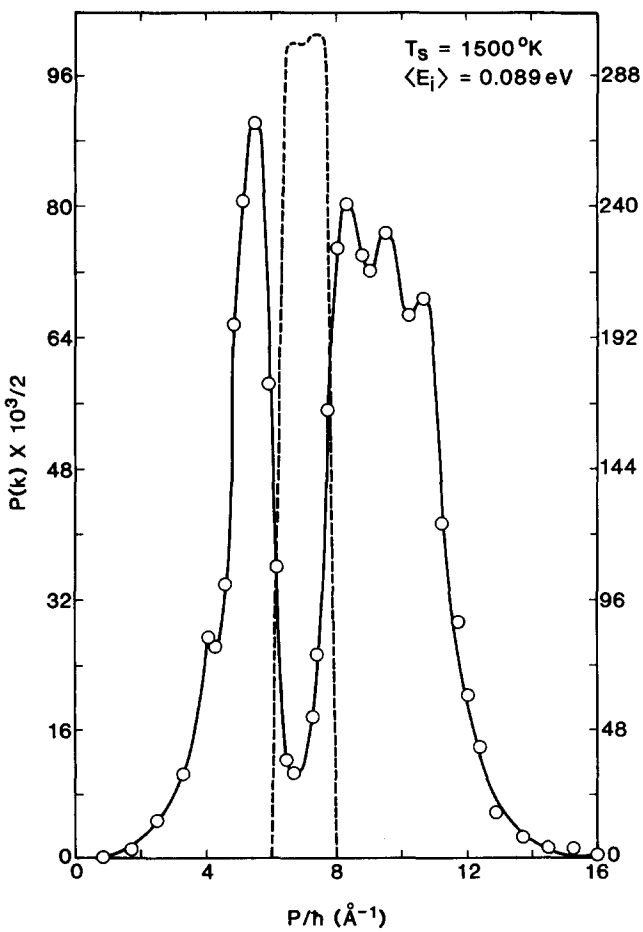

FIG. 11. Surface spectrum for $\theta_i = 0°$ with $T_s = 1500$ K and $\langle E_i \rangle = 0.089$ eV. The dashed curve gives the initial distribution of momenta using the scale on the right of the figure.

a surface phonon spectrum from the Fourier transform of the scattered wave packet. One-, two-, and three-phonon processes are evident in this spectrum.

Within the framework of this semiclassical method, one may easily increase the complexity of the lattice or include lattice defects and/or surface impurities, as desired. Such studies that simulate actual molecular-beam conditions on realistic surfaces are currently in progress.

ACKNOWLEDGMENT

The authors wish to thank the Air Force Office of Scientific Research for financial support of this research under Grant No. AFOSR-82-0311.

[1]For a recent review, see J. C. Tully, Annu. Rev. Phys. Chem. **31**, 319 (1980).
[2]K. C. Janda, J. E. Hurst, C. A. Becker, J. P. Cowin, D. J. Auerbach, and L. Wharton, J. Chem. Phys. 72, 2403 (1980).
[3]S. Adelman and J. D. Doll, J. Chem. Phys. 61, 4242 (1974).
[4]M. Shugard, J. C. Tully, and A. Nitzan, J. Chem. Phys. 66, 2534 (1977).
[5]For example, see J. J. Foster and R. I. Masel, J. Chem. Phys. 75, 2864 (1981).
[6]R. Kumamoto and R. Silbey, J. Chem. Phys. 75, 5164 (1981).
[7]J. Lorenzen and L. M. Raff, J. Chem. Phys. 74, 3929 (1981).
[8]For other excellent examples of semiclassical wave packet methods that likewise replace the study of many classical trajectories, see: E. J. Heller, J. Chem. Phys. 69, 2439 (1979); 65, 4979 (1976); 62, 1544 (1975).
[9]H. F. Harmuth, J. Math. and Phys. 36, 269 (1957).
[10]A. Askar and A. S. Cakmak, J. Chem. Phys. 68, 2794 (1978).
[11]P. M. Agrawal and L. M. Raff, J. Chem. Phys. 74, 5076 (1981).
[12]E. K. Grimmelmann, J. C. Tully, and M. J. Cardillo, J. Chem. Phys. 72, 1039 (1980).